Optics & Laser Technology 91 (2017) 1–6

Contents lists available at ScienceDirect

Optics & Laser Technology

journal homepage: www.elsevier.com/locate/optlastec

Full length article

CW and passively Q-Switched operation of a Ho:YAG waveguide laser

Sean A. McDaniel[a,b,*], Patrick A. Berry[a], Gary Cook[a], David Zelmon[a], Stephanie Meissner[c], Helmuth Meissner[c], Xaiodong Mu[c]

[a] *Air Force Research Laboratory, Sensors Directorate, 2241 Avionics Circle, Wright-Patterson AFB, OH 45433, USA*
[b] *Leidos Inc., 3745 Pentagon Blvd, Beavercreek, OH 45431, USA*
[c] *Onyx Optics Inc., 6551 Sierra Lane, Dublin, CA 94568, USA*

ARTICLE INFO

Keywords:
Solid-state lasers
Infrared lasers
Channeled waveguides
Ho:YAG

ABSTRACT

We report the first demonstration of a Ho: YAG crystal fiber waveguide (CFW) laser operating at 2.09 μm. The CFW structure was produced by adhesive free bonding of holmium doped yttrium aluminum garnet core to an undoped yttrium aluminum garnet cladding. The laser produced CW output powers greater than 500 mW with slope efficiency of 17%. The same crystal when passively Q-switched with Cr: ZnSe, produced pulsed output with energies of 1 μJ at a repetition frequency of 442 kHz.

1. Introduction

In recent years, 2 μm laser sources have seen a growth in utility. Lasers that operate in the 2 μm range, most notably Ho:YAG and Tm:YAG, are considered eye-safe due to the high absorption of light in eye tissue and intraocular fluid. Eye-safe operation, along with several organic absorption lines, drive the need for advancement of 2 μm laser sources, to enable compact, high power systems capable of CW and Q-Switched operation. In this work, we demonstrate the use of Ho:YAG CFW structures to demonstrate a compact laser source, which could be suitable for such applications.

Ho:YAG lasers operating in the 2 μm range have numerous applications including medical [1], dental [2] and as optical pump sources for other laser materials [3–5]. Ho:YAG can easily be pumped by 1.9 μm radiation, usually from a thulium fiber laser [6] or from cross relaxation of a thulium ion under diode pumping at 780 nm in a co-doped crystal. The laser operates on the holmium $^5I_7$-$^5I_8$ [7] transition producing 2.09 μm radiation. This transition has been shown to be active at room temperature [8] and capable of producing high power output.

One approach to guided-wave operation of Ho:YAG laser would be through doping of crystalline YAG fibers [9]. However, high losses in these fibers have so far prevented them from being a viable option for passive or active devices. A more popularized approach is holmium doping of ZBLAN fibers [10,11] or co-doping of holmium and thulium in ZBLAN fibers [12,13]. A maximum output of 6.6 W has been obtained from a Ho:ZBLAN fiber [14]. Additionally, Tm, Ho and co-doped Tm Ho silica fibers have been created with output powers in excess of 80 W [15–19] and are commercially available from vendors including IPG Photonics and NuFern. Direct creation of waveguides in bulk material using ultrafast laser inscription is an approach that was successfully used in YAG [20] and has produced waveguide lasers in Tm:YAG [21]. An alternative approach to guided wave structures using holmium can be realized by adhesive-free bonding (AFB) of a doped YAG core inside of a undoped YAG substrate. This was first used to demonstrate planar waveguides in Tm:YAG but has only recently been successfully demonstrated in a double-clad, fully confined CFW device with Er:YAG [22].

In this paper, we will present the first demonstration of a Ho:YAG CFW laser. Waveguide operation of this material allows for several advantages over bulk operation including improved longitudinal overlap between pump and laser mode, reduced system complexity and increased thermal management properties due to the small active region size and high thermal conductivity of YAG (0.14 $\mathrm{Wcm^{-1}K^{-1}}$) [23].

2. Crystal fiber waveguide construction

The CFW was made from high optical quality single crystal 2 *at.%* Ho:YAG with Onyx Optics adhesive-free bonding technology (AFB). In order to form the desired fiber core size with an undoped YAG cladding, multiple bonding processes with precision milling and polishing processes were applied. Since the trivalent Ho^{3+} ion in YAG occupied the Y^{3+} lattice position that surround by eight oxygen ions, ion diffusion from the Ho:YAG to the un-doped YAG can rarely happen in the CFW fabrication process. The waveguide can be considered to have a perfect step-index profile. The refractive index difference is

---

[*] Corresponding author at: Leidos Inc., 3745 Pentagon Blvd, Beavercreek, OH 45431, USA.
E-mail address: sean.a.mcdaniel@leidos.com (S.A. McDaniel).

http://dx.doi.org/10.1016/j.optlastec.2016.12.004
Received 30 June 2016; Accepted 8 December 2016

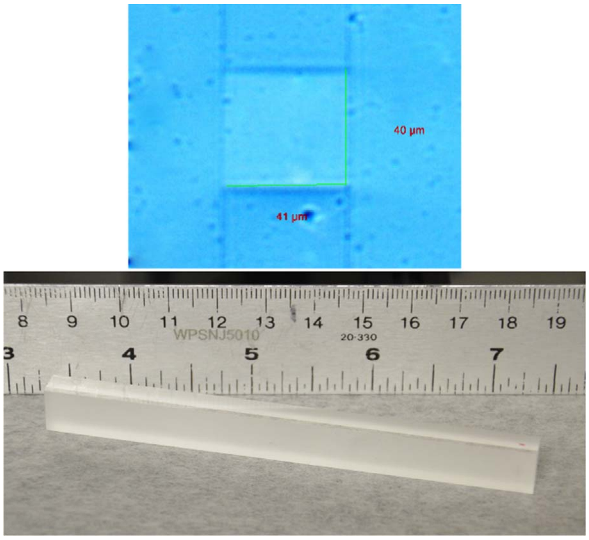

Fig. 1. Ho:YAG waveguide 40 × 40 µm core surrounded by undoped YAG.

around 4.88×10^{-4} as measured by an interferometric method at wavelength of 1.55 µm [24]. The corresponding numerical aperture (NA) was 0.042. We have assumed that the index difference in the core of the waveguide only arises from the inclusion of the holmium dopant. The material dispersion relation in the region of 1.55 – 2 µm is relatively constant, thus the NA of the waveguide at 1.55 µm provides a good estimation of the NA at 2.1 µm.

3. CW experimental setup

The Ho:YAG waveguide consisted of a 40 × 40 µm doped, square core surrounded by undoped YAG, see Fig. 1. The Ho:YAG core of the waveguide was doped to 2 at% and was 100 mm long. The total dimensions of the waveguide crystal were 84 mm×9.8 mm×6.2 mm ($L \times W \times H$). The waveguide was placed on an uncooled mount capable of pitch, yaw and transverse adjustment. We measured the losses of the waveguide using a non-destructive technique, which relies on imaging the scattered light from core of the waveguide [25]. Fitting the scattered light to an exponential provides an upper estimate of the waveguide losses, which were estimated to be 1 dB/cm at 1 µm.

At each end facet of the crystal, flat mirrors were placed to produce a laser cavity. The setup of the waveguide laser can be seen in Fig. 2. This consisted of an isolator (polarizing beam splitter (PBS) and $\lambda/4$ waveplate), a 2.5 cm focal length lens with an NA of 0.16 (L1), a dichroic mirror (M1, highly reflective (HR)@2.1 µm and anti-reflective (AR)@1.9 µm), a variable percentage outcoupler for 2.1 µm (M2), a 2.5 cm focal length collimating lens (L2), and a dichroic beam splitter (DI, HR@2.1 µm and AR@1.9 µm at a 45° angle of incidence). The pump source was an IPG thulium fiber laser (Model TLR-20–1908-LP), which produced a pump spot size of 50 µm. The crystal faces were uncoated, producing a Fresnel reflection of approximately 8%. As a precaution to reduce back reflections into the thulium fiber pump laser, index matching gel was used to decrease the Fresnel reflection. Additionally, the polarizing beam cube and a $\lambda/4$ waveplate were used as an optical isolator.

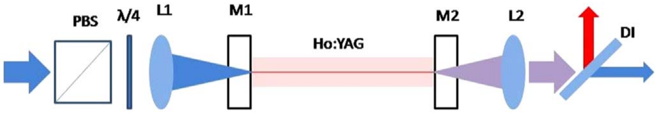

Fig. 2. Waveguide setup of the Ho:YAG waveguide structure.

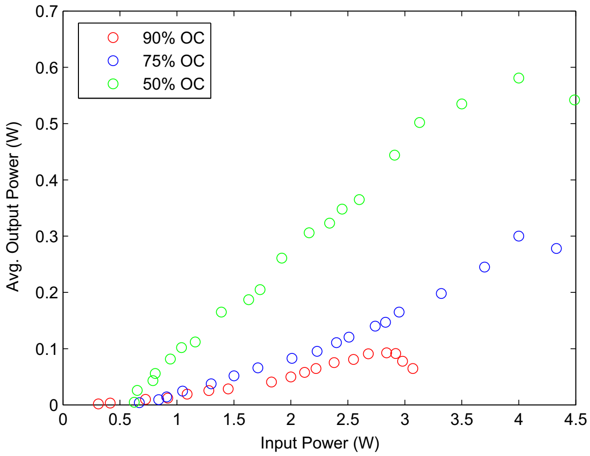

Fig. 3. Waveguide Ho:YAG slope efficiency for 90%, 75% and 50% reflective outcouplers. The output power presented in this graph represents average power on a thermopile power meter.

4. CW results

CW operation of the laser was characterized with 90%, 75% and 50% reflective outcouplers (see Fig. 3). It should be noted that all data was taken while the pump beam was chopped at 20 Hz with a 50% duty cycle in order to decrease the thermal load on the Ho:YAG crystal. The best performing outcoupler, 50% reflective, achieved a slope efficiency of 17% and a threshold of 597 mW. The 75% outcoupler had a slope efficiency of 8% and a threshold of 377 mW. Finally, the 90% outcoupler had a slope efficiency of 1.6% and a threshold of 291 mW.

The non-optimal performance can be attributed to several factors. First, the waveguide laser was uncooled. It has been shown by Barnes et al. [27] that as the temperature increases, laser efficiency decreases in Ho:YAG. The thermal properties of YAG are well characterized, thus using standard thermal transport equations the temperature inside of the waveguide can be modeled using COMSOL(TM). The waveguide structure was modeled as a 40 µm square core located several millimeters away from each face of the CFW. A Gaussian beam with diameter 50 µm was modeled to be incident on the core of the CFW. Using Beer's law absorption, the heat deposition profile was modeled in the waveguide structure. The core of the waveguide had a doping concentration of 2 at%, with an absorption cross section of 1.2×10^{20} cm^2 at 1908 nm. The model calculated a rise in temperature of approximately 52 K for 5 W of incident pump power. From the generated temperature profile, Fig. 4, a parabolic profile was fitted to the temperature gradient. The parabolic profile from Koechner and Bass [28](Eq. (1)) was then used, neglecting stress-dependent variations, to calculated the effective change in index due to the thermal load on the waveguide assuming an absorption depth of 2 cm, see Fig. 5. In Eq. (1), n_0 was the unmodified index, $T(r)$ was the radially dependent temperature, $T(0)$ was the initial temperature and $\frac{dn}{dT}$ was the thermo-optic coefficient for YAG(7.8×10^{-6} K^{-1}).

$$n(r) = n_0 + (T(r) - T(0))\frac{dn}{dT} \tag{1}$$

From Fig. 5, it can be seen that the temperature dependent index profile was approximately flat across the core of the waveguide. From the temperature dependent index profile, beam propagation method (BPM) can be used to test the stability of the waveguide under normal operating conditions, Fig. 6. For the conditions listed in this paper, the propagating mode does not experience significant thermal lensing due to the heat load on the waveguide. Additionally, if the stress-dependent variation in material index was present in the waveguide, an increase in the effective focal length of the material on the order of 20% can be expected [29]. The additional change in refractive index due to the